ATLAS Di-Higgs results

Petar Bokan (DESY), Higgs Hunting 2021
on behalf of the ATLAS Collaboration
September 22, 2021, Orsay and Paris

Outlook

- Introduction
- Non-resonant Higgs boson pair production
- Resonant Higgs boson pair production
- Conclusion

With focus on the most recent results

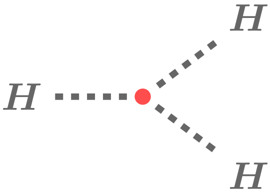

Non-resonant production

SM HH production at the LHC

- Standard Model (SM) predicts **non-resonant** HH production
- Interesting as a direct probe of the **Higgs boson self-coupling**, also $VVHH$ coupling
- Small predicted cross-section in the SM

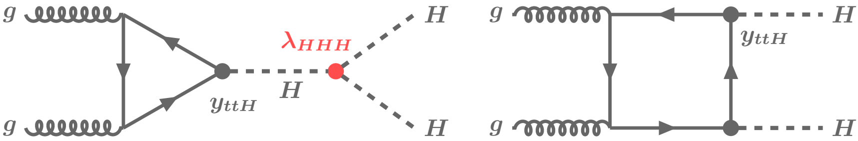

Gluon-gluon fusion (ggF) HH *production,* $31.1^{+2.1}_{-7.2}$ *fb @ 13 TeV* *

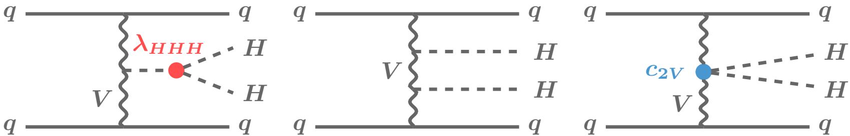

Vector boson fusion (VBF) HH *production,* 1.73 ± 0.04 *fb @ 13 TeV* *

* *Full list of references available at the LHCHXSWGHH website*

Decay channels and public results (non-resonant)

	bb	WW
bb	33% JHEP01(2019)030	
WW	25% JHEP04(2019)092	4.6% JHEP05(2019)124
$\tau\tau$	7.4% ATLAS-CONF-2021-030	2.5%
ZZ	3.1%	1.2%
$\gamma\gamma$	0.26% ATLAS-CONF-2021-016	0.10% EPJC78(2018)1007

27.5 - 36.1 fb^{-1}

139 fb^{-1}

$bbll$ ($l = e$ or μ)
($bbWW$, $bb\tau\tau$, $bbZZ$)
PLB801(2020)135145

Combination
($bbbb$, $bbWW$, $WWWW$, $bb\tau\tau$, $bb\gamma\gamma$ and $WW\gamma\gamma$)
PLB800(2020)135103

HH decay modes and their total relative branching ratios

10.23731/CYRM-2017-002

Limits on the non-resonant HH cross-section assuming the SM kinematics available for the highlighted channels

Decay channels and public results (non-resonant)

	bb	WW
bb	33% JHEP01(2019)030	
WW	25% JHEP04(2019)092	4.6% JHEP05(2019)124
$\tau\tau$	7.4% ATLAS-CONF-2021-030	2.5%
ZZ	3.1%	1.2%
$\gamma\gamma$	0.26% ATLAS-CONF-2021-016	0.10% EPJC78(2018)1007

27.5 - 36.1 fb^{-1} $\leftarrow$ only ggF considered

139 fb^{-1} $\leftarrow$ ggF + VBF considered for $bb\gamma\gamma$ and $bb\tau\tau$

$bbll$ ($l = e$ or μ)
($bbWW$, $bb\tau\tau$, $bbZZ$)
PLB801(2020)135145

Combination
($bbbb$, $bbWW$, $WWWW$, $bb\tau\tau$, $bb\gamma\gamma$ and $WW\gamma\gamma$)
PLB800(2020)135103

HH decay modes and their total relative branching ratios

10.23731/CYRM-2017-002

Limits on the non-resonant HH cross-section assuming the SM kinematics available for the highlighted channels

Decay channels and public results (non-resonant)

	bb	WW
bb	33% JHEP01(2019)030	
WW	25% JHEP04(2019)092	4.6% JHEP05(2019)124
$\tau\tau$	7.4% ATLAS-CONF-2021-030	2.5%
ZZ	3.1%	1.2%
$\gamma\gamma$	0.26% ATLAS-CONF-2021-016	0.10% EPJC78(2018)1007

27.5 - 36.1 fb^{-1} ← only ggF considered

139 fb^{-1} ← ggF + VBF considered for $bb\gamma\gamma$ and $bb\tau\tau$

$bbll$ ($l = e$ or μ) ($bbWW$, $bb\tau\tau$, $bbZZ$) PLB801(2020)135145

Combination ($bbbb$, $bbWW$, $WWWW$, $bb\tau\tau$, $bb\gamma\gamma$ and $WW\gamma\gamma$) PLB800(2020)135103

HH decay modes and their total relative branching ratios

10.23731/CYRM-2017-002

Limits on the non-resonant HH cross-section assuming the SM kinematics available for the highlighted channels

Constraints on $\kappa_\lambda = \lambda_{HHH}/\lambda_{HHH}^{\mathrm{SM}}$ ($bbbb$, $bb\tau\tau$ and $bb\gamma\gamma$)

Additionally, constraints on $\kappa_{2V} = c_{2V}/c_{2V}^{\mathrm{SM}}$ ($bbbb$, 126 fb^{-1}) JHEP07(2020)108

See Tatjana's talk

$HH \to b\bar{b}\tau^+\tau^-$ (139 fb^{-1})

- Final states considered: $\tau_{\mathrm{had}}\tau_{\mathrm{had}}$ and $\tau_{\mathrm{lep}}\tau_{\mathrm{had}}$ (lep/had = leptonic/hadronic τ lepton decay)
- Three signal regions (SRs) based on the di-τ decay mode and trigger category (single-e/μ, τ_{had} triggers, and $e/\mu + \tau_{\mathrm{had}}$ triggers)
- Majority of backgrounds with jets misidentified as τ_{had} estimated using data-driven techniques
- Backgrounds with true-τ_{had} simulated ($t\bar{t}$ and $Z \to \tau\tau + bb$ norms freely floated in the final fit)
- Multivariate analysis (MVA) classifiers used to distinguish the signal from backgrounds
- MVA scores used as final discriminants in the fit

ATLAS-CONF-2021-030

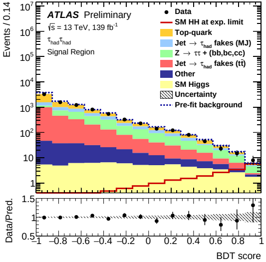

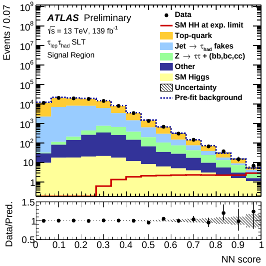

See Tatjana's talk

$HH \to b\bar{b}\tau^+\tau^-$ (139 fb^{-1})

- Final states considered: $\tau_{\rm had}\tau_{\rm had}$ and $\tau_{\rm lep}\tau_{\rm had}$ (lep/had = leptonic/hadronic τ lepton decay)
- Three signal regions (SRs) based on the di-τ decay mode and trigger category (single-e/μ, $\tau_{\rm had}$ triggers, and $e/\mu + \tau_{\rm had}$ triggers)
- Majority of backgrounds with jets misidentified as $\tau_{\rm had}$ estimated using data-driven techniques
- Backgrounds with true-$\tau_{\rm had}$ simulated ($t\bar{t}$ and $Z \to \tau\tau + bb$ norms freely floated in the final fit)
- Multivariate analysis (MVA) classifiers used to distinguish the signal from backgrounds
- MVA scores used as final discriminants in the fit

95% CL limit on $\sigma_{HH}/\sigma_{HH}^{\rm SM}$ (ggF + VBF):

-1σ	Expected	$+1\sigma$	Observed
2.8	3.9	5.4	4.7

ATLAS-CONF-2021-030

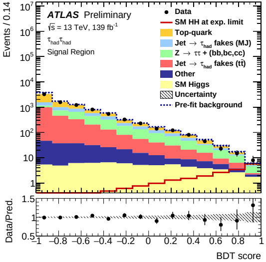

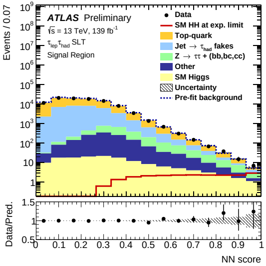

See Tatjana's talk

$HH \to b\bar{b}\tau^+\tau^-$ (139 fb^{-1})

- Final states considered: $\tau_{\text{had}}\tau_{\text{had}}$ and $\tau_{\text{lep}}\tau_{\text{had}}$ (lep/had = leptonic/hadronic τ lepton decay)
- Three signal regions (SRs) based on the di-τ decay mode and trigger category (single-e/μ, τ_{had} triggers, and $e/\mu + \tau_{\text{had}}$ triggers)

Results almost twice better than what would be expected from just the increased dataset w.r.t. the previous paper PRL 121(2018)191801 (exp. 14.8, obs. 12.7) due to improved reconstruction and identification techniques, new triggers and a number of analysis-specific improvements

95% CL limit on $\sigma_{HH}/\sigma^{\text{SM}}_{HH}$ (ggF + VBF):

-1σ	Expected	$+1\sigma$	Observed
2.8	3.9	5.4	4.7

ATLAS-CONF-2021-030

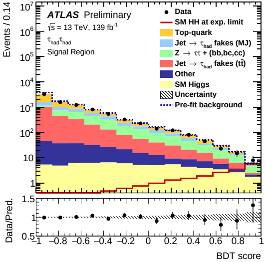

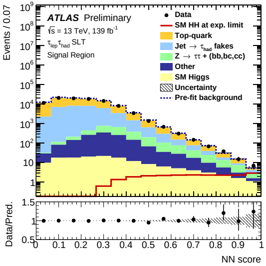

See Raphael's talk

$HH \to b\bar{b}\gamma\gamma$ (139 fb^{-1})

- Event selection based on di-photon triggers
- Events split into low- and high-mass SRs
  - Low-mass region sensitive to large $|\kappa_\lambda|$
  - High-mass region sensitive to the SM signal and small $|\kappa_\lambda|$
- Signal and single-Higgs background $m_{\gamma\gamma}$ shapes modelled with a double-sided Crystal Ball function
- Continuum di-photon background modelled using an exponential functional form (by fitting the data in the sidebands)
- Boosted decision trees trained on $\kappa_\lambda = 1$ and 10 signals in the high- and low-mass SRs, respectively.
- Loose and tight BDT score categories defined

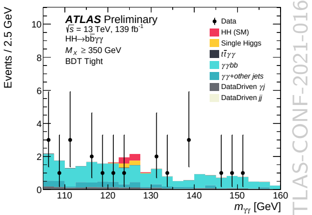

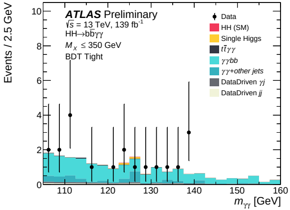

Results are extracted from a fit of the $m_{\gamma\gamma}$ distributions in the range $105 < m_{\gamma\gamma} < 160$ GeV

See Raphael's talk

$HH \to b\bar{b}\gamma\gamma$ (139 fb^{-1})

- Event selection based on di-photon triggers
- Events split into low- and high-mass SRs
  - Low-mass region sensitive to large $|\kappa_\lambda|$
  - High-mass region sensitive to the SM signal and small $|\kappa_\lambda|$
- Signal and single-Higgs background $m_{\gamma\gamma}$ shapes modelled with a double-sided Crystal Ball function
- Continuum di-photon background modelled using an exponential functional form (by fitting the data in the sidebands)
- Boosted decision trees trained on $\kappa_\lambda = 1$ and 10 signals in the high- and low-mass SRs, respectively.
- Loose and tight BDT score categories defined

95% CL limit on $\sigma_{HH}/\sigma_{HH}^{\mathrm{SM}}$ (ggF + VBF):

Expected	Observed
5.5	4.1

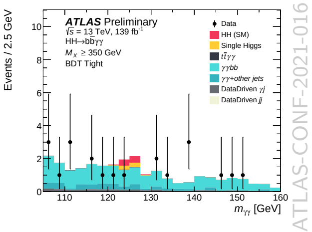

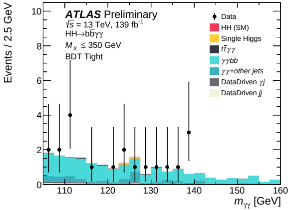

Results are extracted from a fit of the $m_{\gamma\gamma}$ distributions in the range $105 < m_{\gamma\gamma} < 160$ GeV

See Raphael's talk

$HH \to b\bar{b}\gamma\gamma$ (139 fb^{-1})

- Event selection based on di-photon triggers
- Events split into low- and high-mass SRs
  - Low-mass region sensitive to large $|\kappa_\lambda|$
  - High-mass region sensitive to the SM signal and small $|\kappa_\lambda|$
- Signal and single-Higgs background $m_{\gamma\gamma}$ shapes modelled with a double-sided Crystal Ball function

Results almost three times better than what would be expected from just the increased dataset w.r.t. the previous paper JHEP11(2018)040 (exp 28, obs 22) due to low- and high-mass SR categorisation, multivariate events selection and other analysis optimisations

95% CL limit on $\sigma_{HH}/\sigma_{HH}^{\mathrm{SM}}$ (ggF + VBF):

Expected	Observed
5.5	4.1

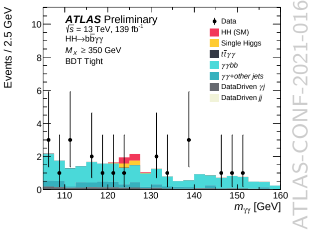

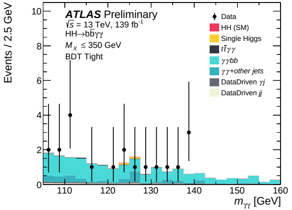

Results are extracted from a fit of the $m_{\gamma\gamma}$ distributions in the range $105 < m_{\gamma\gamma} < 160$ GeV

$HH \to b\bar{b}\gamma\gamma$ (139 fb^{-1})

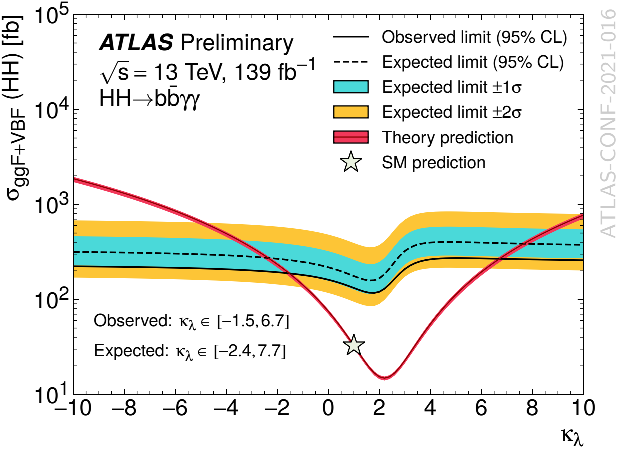

	Expected	Observed
$bb\gamma\gamma$ 139 fb^{-1} (ggF + VBF)	$\kappa_\lambda \in [-2.4, 7.7]$	$\kappa_\lambda \in [-1.5, 6.7]$

at 95% CL

$HH \to b\bar{b}\gamma\gamma$ (139 fb^{-1})

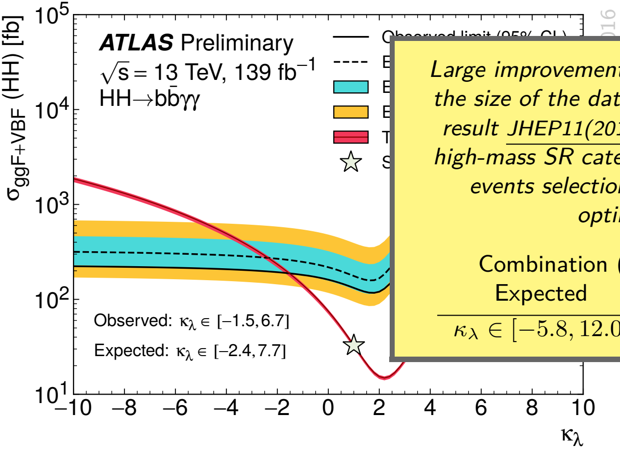

Large improvement beyond the increase in the size of the dataset w.r.t. the previous result JHEP11(2018)040 due to low- and high-mass SR categorisation, multivariate events selection and other analysis optimisations

Combination (27.5 – 36.1 fb^{-1}):

Expected	Observed
$\kappa_\lambda \in [-5.8, 12.0]$	$\kappa_\lambda \in [-5.0, 12.0]$

	Expected	Observed
$bb\gamma\gamma$ 139 fb^{-1} (ggF + VBF)	$\kappa_\lambda \in [-2.4, 7.7]$	$\kappa_\lambda \in [-1.5, 6.7]$

at 95% CL

Limits on $\sigma_{HH}/\sigma_{HH}^{SM}$: summary

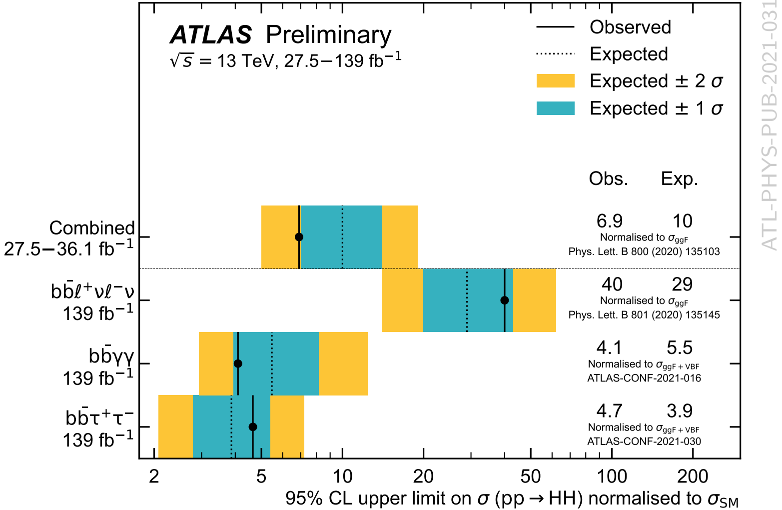

VBF $HH \to b\bar{b}b\bar{b}$ (126 fb^{-1})

- Analysis optimized to search for VBF HH production
- Multijet background constitute about 95% of the total background (data-driven)
- $t\bar{t}$ background simulated, normalisation of all-hadronic $t\bar{t}$ determined from data
- ggF HH production normalised to the SM expectation and treated as background

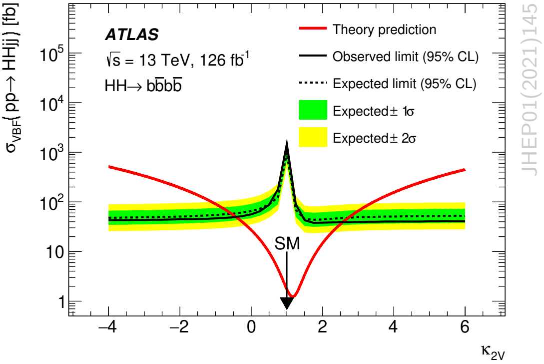

95% CL limit on $\sigma_{\text{VBF}}/\sigma_{\text{VBF}}^{\text{SM}}$

Expected	Observed
550	840

Allowed κ_{2V} interval at 95% CL

Expected	Observed
$[-0.55, 2.72]$	$[-0.43, 2.56]$

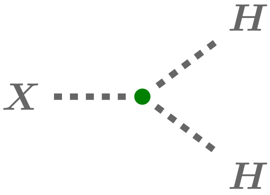

Resonant production

$m_X > 2 \times m_H$

Resonant HH production at the LHC

- Main focus on resonant ggF HH production
- Results based on the full Run 2 dataset available for $bbbb$, $bb\tau\tau$ and $bb\gamma\gamma$ channels

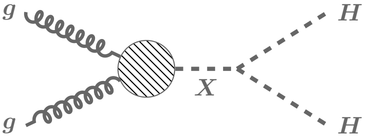

Resonant ggF HH production

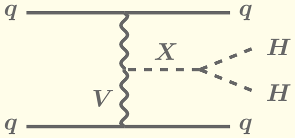

Resonant VBF HH production

$bbbb$, 126 fb^{-1}
JHEP07(2020)108

Typical benchmark hypotheses considered in the ATLAS publications:

- Narrow-width spin $= 0$ resonance
- Kaluza-Klein graviton in the bulk Randall–Sundrum model (spin $= 2$)

Resonant $HH \to b\bar{b}b\bar{b}$ (126 – 139 fb^{-1})

Resolved

- $m_X \in [251, 1500]$ GeV
- b-jet, b-jet + jet and H_T ($\sum_{\text{jets}} |E_T|$) triggers
- BDTs used to pair b-jets
- Fully data-driven background estimation ($\sim 95\%$ multijet, rest $t\bar{t}$)
  Neural-network reweighting correction applied

Boosted

- $m_X \in [900, 3000]$ GeV
- Large-radius jet triggers
- At least two large-radius jets required
- Considers $2b$, $3b$ and $4b$ categories (large-radius jet matched to 1 or 2 b-tagged track jets)
- Fully data-driven multijet background estimation
- $t\bar{t}$ background simulated (corrections applied in the $2b$ and $3b$ categories)

ATLAS-CONF-2021-035

Resolved

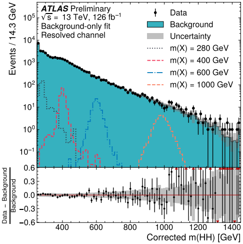

Boosted, $4b$

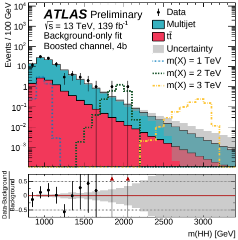

Resonant $HH \to b\bar{b}b\bar{b}$ (126 – 139 fb^{-1})

SRs defined in the $(m(H_1), m(H_2))$ plane

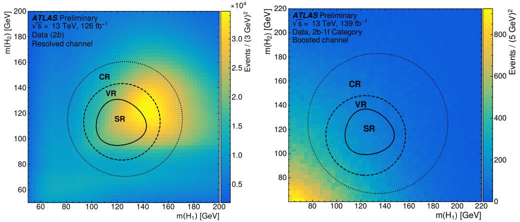

- Final discriminant: (corrected) m_{HH}

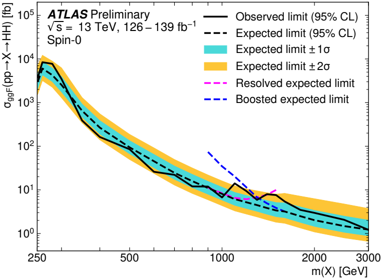

spin-0

ATLAS-CONF-2021-035

Resolved

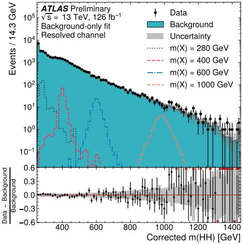

Boosted, $4b$

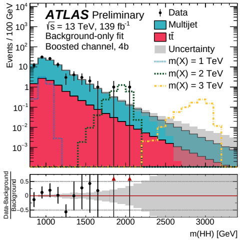

Resonant $HH \to bb\tau\tau/bb\gamma\gamma$ (139 fb^{-1})

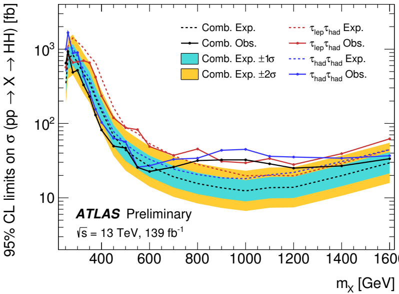

$X \to HH \to b\bar{b}\tau^+\tau^-$, Resolved

ATLAS-CONF-2021-030

$\tau_{\text{had}}\tau_{\text{had}}$ and $\tau_{\text{lep}}\tau_{\text{had}}$

– Similar strategy to the non-resonant analysis

– Parametric neural networks (PNNs) used to distinguish signals from background

– Final discriminants: PNN(m_{HH}) scores

Resonant $HH \to bb\tau\tau/bb\gamma\gamma$ (139 fb^{-1})

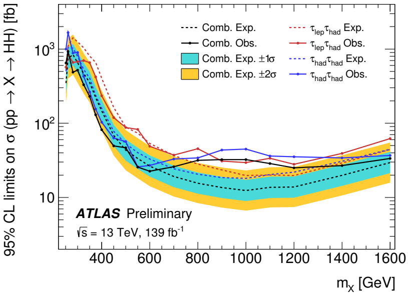

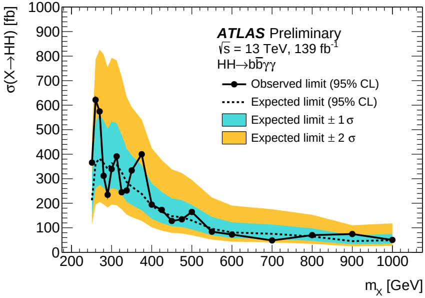

$X \to HH \to b\bar{b}\tau^+\tau^-$, Resolved

ATLAS-CONF-2021-030

$\tau_{\mathrm{had}}\tau_{\mathrm{had}}$ and $\tau_{\mathrm{lep}}\tau_{\mathrm{had}}$

– *Similar strategy to the non-resonant analysis*
– *Parametric neural networks (PNNs) used to distinguish signals from background*
– *Final discriminants: PNN(m_{HH}) scores*

$X \to HH \to b\bar{b}\gamma\gamma$

ATLAS-CONF-2021-016

– *BDTs trained separately against $\gamma\gamma$ and single-H backgrounds, then combined in quadrature*
– *BDTs and $m^*_{b\bar{b}\gamma\gamma}$ used to select events*
– *Final discriminants: $m_{\gamma\gamma}$ distributions*

Resonant spin-0 limits: summary

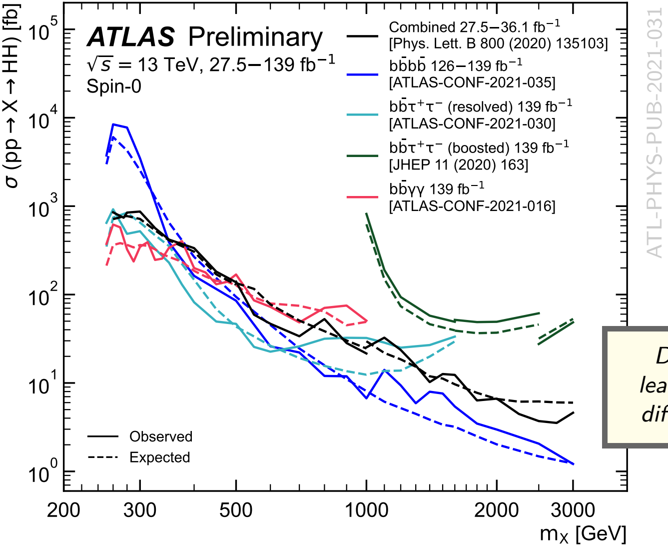

Different channels lead the sensitivity in different m_X regions

Resonant $HH \to b\bar{b}b\bar{b}$ (spin-2, 139 fb^{-1})

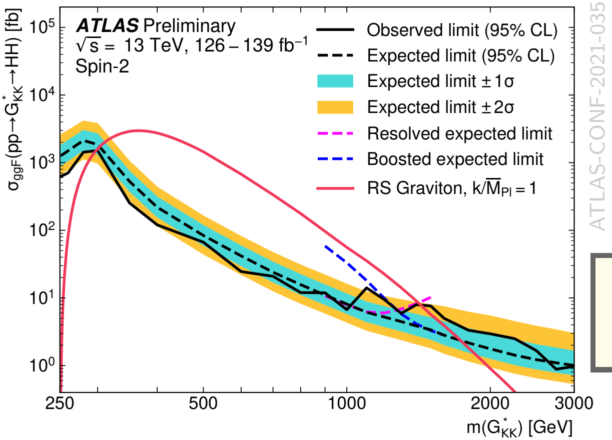

Previous combined exclusion:

310 – 1380 GeV

PLB800(2020)135103

- Bulk Randall–Sundrum model excluded for graviton masses between 298 and 1440 GeV $(k/\bar{M}_{\mathrm{Pl}} = 1)$ at 95% CL

Conclusion

- New results
  - $bbbb$ (resonant)
  - $bb\tau\tau$ (resonant, limits on non-resonant ggF + VBF cross-section)
  - $bb\gamma\gamma$ (resonant, limits on non-resonant ggF + VBF cross-section, κ_λ constraints)
- Large sensitivity improvements compared to the previous iterations

Other interesting results (based on partial Run 2 dataset):

- *ATLAS-CONF-2019-049*
  Constraints on κ_λ from the combination of H and HH production analyses
- *Phys.Let.B 800(2020)135103*
  Constraints on the hMSSM and EWK-singlet models from HH analyses
- *ATL-PHYS-PUB-2018-053*
  HL-LHC prospects ($bbbb$, $bb\tau\tau$ and $bb\gamma\gamma$)

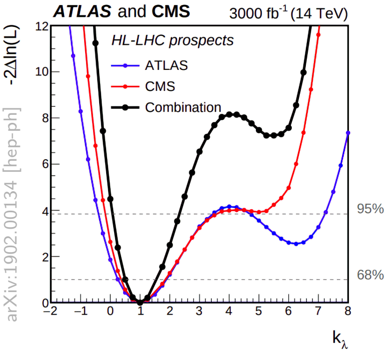

Thank you for your attention

Backup

Combined results (27.5 – 36.1 fb^{-1})

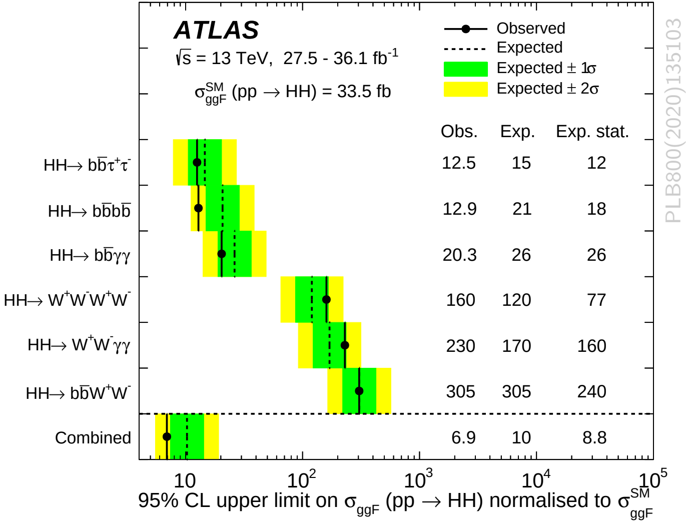

Combined results (27.5 – 36.1 fb^{-1})

Several new results available based on the full Run 2 dataset

New result available →

New result available →

New result available $bb\ell\ell$ $(\ell = e/\mu)$

($bbWW$, $bb\tau\tau$ and $bbZZ$)

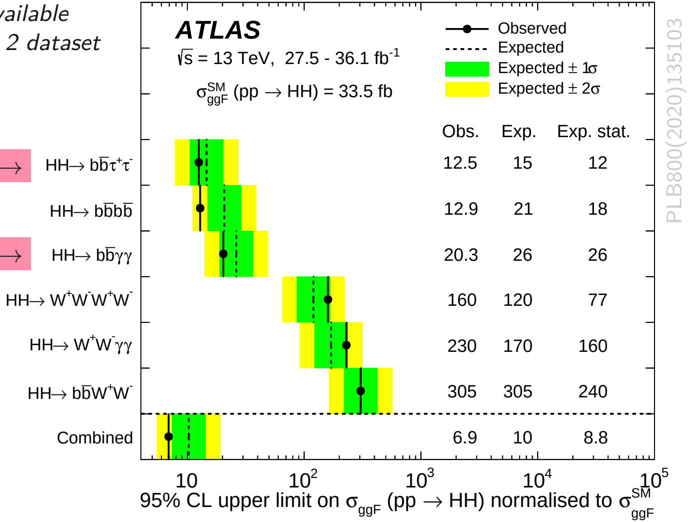

Combined κ_λ results (27.5 – 36.1 fb^{-1})

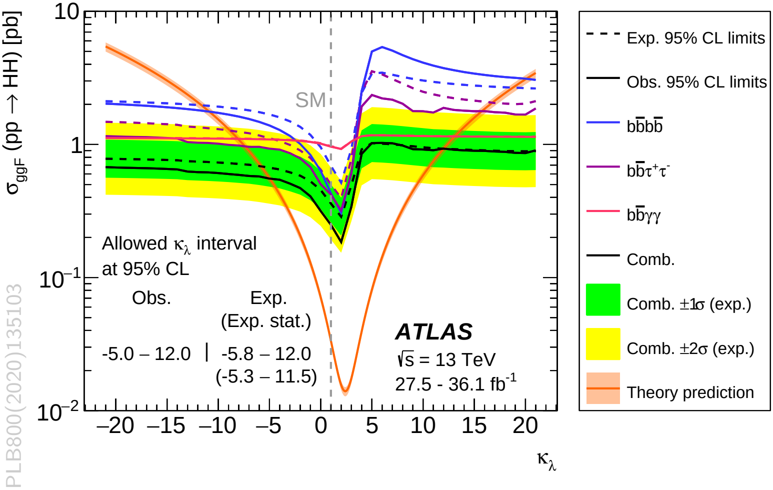

Expected	Observed
$\kappa_\lambda \in [-5.8, 12.0]$	$\kappa_\lambda \in [-5.0, 12.0]$

at 95% CL

Combined κ_λ results (27.5 – 36.1 fb^{-1})

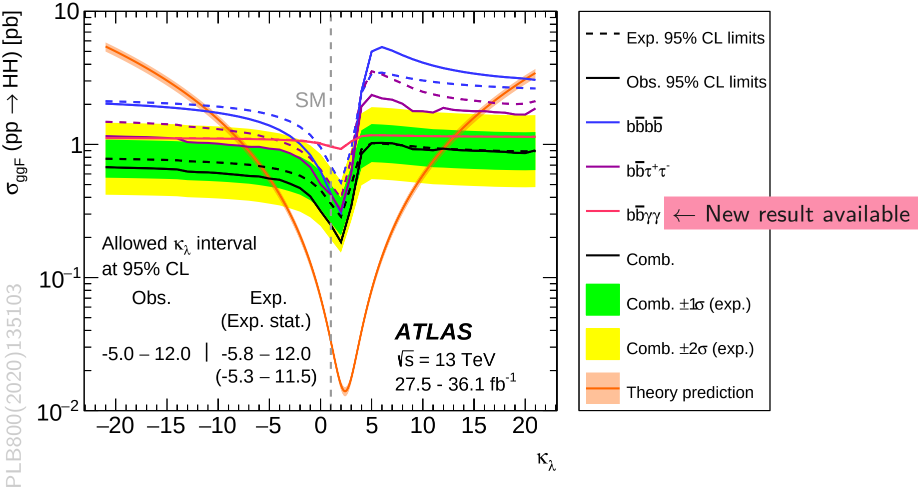

Expected	Observed
$\kappa_\lambda \in [-5.8, 12.0]$	$\kappa_\lambda \in [-5.0, 12.0]$

at 95% CL

Resonant $HH \to bb\tau\tau$ (139 fb^{-1})

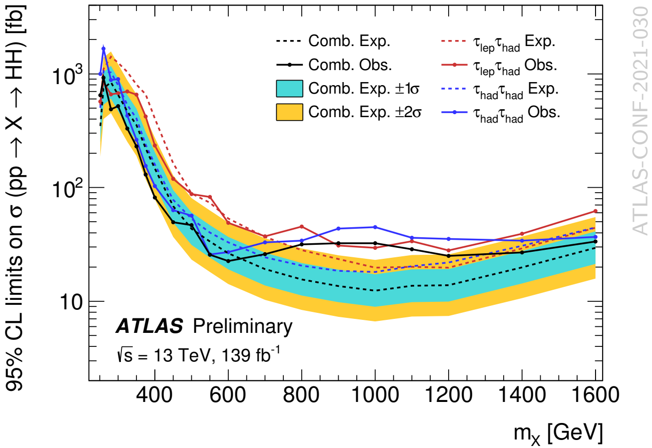

- The largest excess observed at 1 TeV, with a local (global) significance of 3.0σ $(2.0^{+0.4}_{-0.2}\sigma)$
- Largest local significance for $\tau_{\rm had}\tau_{\rm had}$ $(\tau_{\rm lep}\tau_{\rm had})$ channel: 2.8σ (1.5σ) at 1 TeV (1.1 TeV)

Resonant $HH \rightarrow bbbb$ (139 fb^{-1})

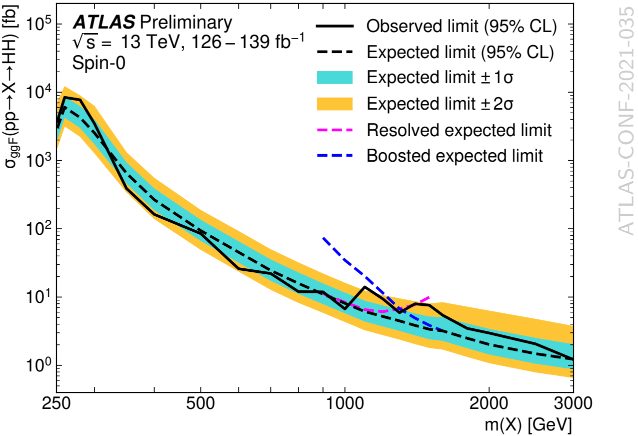

- The largest excess observed at 1.1 TeV, with a local (global) significance of 2.6σ (1.0σ)
- Spin-2: local (global) significance of 2.7σ (1.2σ)